



NIH Public Access

Author Manuscript

Epilepsia. Author manuscript; available in PMC 2013 November 01.

Published in final edited form as:

Epilepsia. 2012 November ; 53(0 6): 22–30. doi:10.1111/j.1528-1167.2012.03699.x.

Impaired neurovascular coupling to ictal epileptic activity and spreading depolarization in a patient with subarachnoid hemorrhage: Possible link to blood–brain barrier dysfunction

Maren K. L. Winkler*, Yoash Chassidim†,‡, Svetlana Lublinsky†,‡, Gajanan S. Revankar*, Sebastian Major*,§,¶, Eun-Jeung Kang*,¶, Ana I. Oliveira-Ferreira*,¶, Johannes Woitzik#, Nora Sandow#, Michael Scheel**, Alon Friedman†, and Jens P. Dreier*,§,¶

*Center for Stroke Research Berlin, Charité University Medicine Berlin, Berlin, Germany

†Department of Physiology and Neurobiology, Zlotowski Center for Neuroscience, Ben-Gurion University of the Negev, Beer- Sheva, Israel

‡Department of Neuroradiology, Soroka University Medical Center and Zlotowski Center for Neuroscience, Ben-Gurion University of the Negev, Beer-Sheva, Israel

§Department of Neurology, Charité University Medicine Berlin, Berlin, Germany

¶Department of Experimental Neurology, Charité University Medicine Berlin, Berlin, Germany

#Department of Neurosurgery, Charité University Medicine Berlin, Berlin, Germany

**Department of Neuroradiology, Charité University Medicine Berlin, Berlin, Germany

SUMMARY

Spreading depolarization describes a sustained neuronal and astroglial depolarization with abrupt ion translocation between intraneuronal and extracellular space leading to a cytotoxic edema and silencing of spontaneous activity. Spreading depolarizations occur abundantly in acutely injured human brain and are assumed to facilitate neuronal death through toxic effects, increased metabolic demand, and inverse neurovascular coupling. Inverse coupling describes severe hypoperfusion in response to spreading depolarization. Ictal epileptic events are less frequent than spreading depolarizations in acutely injured human brain but may also contribute to lesion progression through increased metabolic demand. Whether abnormal neurovascular coupling can occur with ictal epileptic events is unknown. Herein we describe a patient with aneurysmal subarachnoid hemorrhage in whom spreading depolarizations and ictal epileptic events were measured using subdural opto-electrodes for direct current electrocorticography and regional cerebral blood flow recordings with laser-Doppler flowmetry. Simultaneously, changes in tissue partial pressure of oxygen were recorded with an intraparenchymal oxygen sensor. Isolated spreading depolarizations and clusters of recurrent spreading depolarizations with persistent depression of spontaneous activity were recorded over several days followed by a status epilepticus. Both spreading depolarizations and ictal epileptic events were accompanied by hyperemic blood flow responses at one optode but mildly hypoemic blood flow responses at another. Of note, quantitative analysis of Gadolinium-diethylene-triamine-pentaacetic acid

© 2012 International League Against Epilepsy *Epilepsia*,

Address correspondence to: Jens P. Dreier, Center for Stroke Research, Campus CharitéMitte, Charité University Medicine Berlin, Charitéplatz 1, 10117 Berlin, Germany. jens.dreier@charite.de.

Disclosures

The authors have no financial interest in this manuscript and no affiliations (relationships) to disclose. The authors confirm that they have read the Journal's position on issues involved in ethical publication and affirm that this report is consistent with those guidelines.

(DTPA)-enhanced magnetic resonance imaging detected impaired blood–brain barrier integrity in the region where the optode had recorded the mildly hypoemic flow responses. The data suggest that abnormal flow responses to spreading depolarizations and ictal epileptic events, respectively, may be associated with blood–brain barrier dysfunction.

Keywords

Status epilepticus; Spreading depression; Subarachnoid hemorrhage; Blood–brain barrier; Electrocorticography

Spreading depolarization (SD) is a wave of massive ion translocation between the intracellular and extracellular space, near-complete sustained depolarization of neurons, glial depolarization, neuronal swelling, distortion of dendritic spines, and an abrupt, large, negative change of the slow electrical potential (Dreier, 2011). By contrast, epileptic activity is characterized by a milder sustained depolarization with less pronounced disturbance of ion homeostasis up to the so-called ceiling level (Heinemann & Lux, 1977). Whereas the sustained depolarization remains below the inactivation threshold for the generation of action potentials during epileptic activity, this threshold is exceeded during SD. Therefore, during epileptic events, neurons typically fire synchronously action potentials at a high frequency while silencing (spreading depression) of spontaneous activity is observed during SD (Kager et al., 2002).

Convulsive and nonconvulsive seizures frequently occur in acute brain injuries such as aneurysmal subarachnoid hemorrhage (aSAH) or traumatic brain injury (TBI), and these are associated with unfavorable outcome (Vespa et al., 1999; Butzkueven et al., 2000; Claassen et al., 2003; Buczacki et al., 2004). Recent electrocorticography (ECoG) recordings from human patients with aSAH or TBI demonstrate that SDs are more frequent compared to seizures (Fabricius et al., 2008; Dreier et al., 2012) and are associated with worse outcomes as well (Hartings et al., 2011a; Dreier et al., 2012).

Both epileptic activity and SD lead to metabolic stress that is the more deleterious the longer they last (Dreier, 2011). Therefore, potent mechanisms exist limiting the duration of these pathologic events. However, energy is required for a number of these mechanisms. This applies particularly to the additional recruitment of sodium-potassium pump activity. Therefore, to increase energy delivery as well as clearance of the tissue from metabolites, regional cerebral blood flow (rCBF) normally rises during both epileptic activity and SD (Zhao et al., 2007; Sukhotinsky et al., 2010). Such rCBF increases in response to epileptic activity or SD share a number of mechanisms with the neurovascular coupling to physiologic neuronal activation (Attwell & Iadecola, 2002; Koehler et al., 2009), but the changes are more pronounced (Dreier, 2011). Therefore, rCBF rises by 100% during SD under normal conditions. This spreading hyperemia outlasts the tissue depolarization by about 1 min. Thereafter, rCBF mildly declines for up to 2 h, a process referred to as spreading oligemia (Piilgaard & Lauritzen, 2009). However, under pathologic conditions such as exposure of the cortex to erythrocyte products in the subarachnoid space, SDs can cause severe hypoemia advancing to ischemia instead of the protective spreading hyperemia by inverse neurovascular coupling (Dreier, 2011). Such SD-induced ischemia is characterized by the propagation of the perfusion deficit together with the depolarization wave in the tissue (=spreading ischemia). As a consequence of (1) the mismatch between energy demand and supply and (2) the disturbed extracellular clearance of metabolites, the SD is prolonged, thereby increasing the risk for neuronal injury. Whether the neurovascular response to epileptic activity can be inverted in a similar fashion is largely unknown. Herein we report on a patient with aSAH, in whom we found hypoemic rCBF responses to both

ictal epileptic activity and SD. Of interest, these abnormal neurovascular responses were locally restricted to an area with blood–brain barrier (BBB) dysfunction. This finding is interesting because the anatomic overlaps alone suggest that pathologic changes that disturb neurovascular responses may also lead to dysfunction of the BBB and vice versa. Thus three different cell types essentially constitute the BBB: endothelial cells, pericytes, and astrocytes (Abbott et al., 2006; Neuwelt et al., 2011). Neurovascular coupling is regulated on the level of resistance arterioles and capillaries. It involves the coordinated action of neurons, astrocytes, endothelial cells, pericytes, and vascular smooth muscle cells. Together all these cells form the neurovascular unit.

Methods

The patient was recruited at the Charité Campus Virchow (Charité University Medicine Berlin) for the Co-Operative Studies of Brain Injury Depolarizations (COSBID, see <http://www.cosbid.org>). The research protocol was approved by the local ethics committee. Clinical and research consents were obtained according to the Declarations of Helsinki and Tokyo.

Recording of neuromonitoring data

A linear, six-contact platinum ECoG recording strip (Wyler, 5-mm diameter; Ad-Tech Medical, Racine, WI, U.S.A.) was placed on cerebral cortex accessible through the craniotomy (right frontal cortex) during aneurysm surgery as described previously (Dreier et al., 2006). For the measurement of rCBF with laser-Doppler flowmetry (LDF), four optodes were integrated in the electrode strip neighboring the electrodes 3, 4, 5, and 6 (Perimed AB, Järfälla, Sweden) (Dreier et al., 2009). For the assessment of the tissue partial pressure of oxygen ($p_{ti}O_2$), a Clark-type intraparenchymal oxygen sensor (Licox CC1-SB; Integra Lifesciences Corporation, Plainsboro, NJ, U.S.A.) was placed near electrodes 3 and 4 of the electrode strip. This thin probe with a diameter of 0.5 mm, samples $p_{ti}O_2$ of cortical and subcortical tissues within a radius between 7 and 15 mm² (Nortje & Gupta, 2006).

The ECoG was recorded continuously in five active channels from the six-electrode linear array subdural electrode strip. Electrode 1 served as ground, electrodes 2–6 (interelectrode distance 1 cm) were connected in sequential bipolar fashion to a GT205 amplifier (0.01–45 Hz) (ADI Instruments, Bella Vista, NSW, Australia). Moreover, each electrode was referenced to an ipsilateral subdermal platinum electrode (SpesMedica, Battipaglia, Italy). Parallel recording of the direct current (DC)-ECoG was performed using a BrainAmp amplifier (0–45 Hz) (BrainProducts GmbH, Munich, Germany). Data were sampled at 200 Hz and recorded and analyzed with a Powerlab 16/SP analog/digital converter, CHART-7 software (ADI Instruments), and BrainVision Recorder software (BrainProducts GmbH).

Analysis of neuromonitoring data

SD was defined by the sequential onset in adjacent channels of a slow potential change in the near-DC/alternating current (AC)-ECoG (bandwidth 0.01–45 Hz) that propagated along the electrode strip (Dreier et al., 2006; Fabricius et al., 2006). The corresponding spreading depression of brain electrical activity was observed as a rapid reduction in ECoG power. The power of the bandpass- filtered ECoG (bandwidth 0.01–45 Hz) was used for visual enhancement of the amplitude loss during spreading depression, and the integral of power (bandpass 0.5–45 Hz) to determine the duration of the depression period, starting with the initial decrease and ending with the start of the recovery phase (Dreier et al., 2006). The duration of the SD-induced depression of activity was assessed separately for all individual channels involved. Slow potential changes that indicated SD while the AC-ECoG band was isoelectric were defined as isoelectric SDs (Hartings et al., 2011b). Ictal epileptic activity

was defined as rhythmic discharges with spikes, polyspikes, or sharp waves of at least 10-s duration (Fabricius et al., 2008; Dreier et al., 2012). rCBF and $p_{ti}O_2$ were continuously analyzed as reported previously (Dreier et al., 2009; Bosche et al., 2010). Data are given as median (first, third quartiles).

Assessment of BBB dysfunction with magnetic resonance imaging

Quantitative analysis of gadolinium-diethylene-triamine-pentaacetic acid (Gd-DPTA)-enhanced magnetic resonance imaging (MRI) was performed using a semiquantitative approach, based on Tomkins et al. (2001). Briefly summarized, the difference of enhancement values in paired, matching brain images was compared before and after Gd-DPTA administration. The percent difference of enhancement values for the postcontrast T1-weighted images with respect to the precontrast images were calculated as $100 * (\text{intensity}_{\text{post}} - \text{intensity}_{\text{pre}}) / \text{intensity}_{\text{pre}}$. In addition, matching regions of 3×3 pixels were statistically compared in precontrast versus postcontrast images using unpaired *t*-test with false discovery rate (FDR) correction to create a significance level map indicating regions with significant enhancement differences. The percent difference and significance maps were then used to create an image showing brain regions with percent differences between 20% and 100% and significance level of $p < 0.05$. Changes in signal enhancement were considered to be due to BBB dysfunction if they occurred within the brain parenchyma.

Case report

The 71-year-old man presented with a World Federation of Neurological Surgeons (WFNS) grade 5 aSAH caused by a 4-mm aneurysm of the anterior communicating artery. The initial CT scan revealed a Fisher grade 4 aSAH associated with intraparenchymal hemorrhage in the right frontal lobe and a marked intraventricular hemorrhage leading to internal hydrocephalus. The aneurysm was surgically clipped, and extraventricular drainage was established. The optoelectrode strip for the ECoG and rCBF recordings and the oxygen sensor were placed on the right frontal cortex. The patient was transferred to the intensive care unit. He was artificially ventilated; mean arterial pressure (MAP) and intracranial pressure (ICP) were monitored continuously. Sedation was maintained with propofol throughout the monitoring period (except for days 2, 6, 11, and 12). In addition midazolam, fentanyl, and remifentanil were administered on days 0, 1, and 7. Glasgow Coma Scale score (GCS), blood gases, glucose, and electrolytes were assessed every 6 h. A thorough neurologic examination was performed daily. There were no clinical signs of delayed cerebral ischemia throughout the monitoring period. Daily transcranial Doppler sonography was performed at the bedside. Mean blood flow velocities remained below 120 cm/s for both middle cerebral arteries throughout the observation period. The absence of proximal vasospasm was confirmed by digital subtraction angiography (DSA) on day 7. Two MRI studies, performed on days 11 and 15 after the initial hemorrhage, did not show evidence of cerebral infarction.

Adverse events during the monitoring period included elevated ICP values starting on day 2. On day 4, chest x-ray showed bilateral infiltration in the lower lung fields, suggesting pneumonia. On the following day, the patient developed fever. In addition, a urinary tract infection caused by *Proteus mirabilis* was diagnosed. Body temperature and leukocyte count decreased on day 7 after the initiation of antibiotic treatment (cotrimoxazole). On day 12, the nursing staff noted spells associated with breath-holding that were interpreted as epileptic seizures consistent with the ECoG showing ictal epileptic activity. Therefore, treatment with levetiracetam was initiated. After the monitoring, the electrode strip was removed by gentle traction. No hemorrhagic or infectious complications of the electrode strip were encountered.

The patient was discharged from the intensive care unit with a ventriculoperitoneal shunt and a percutaneous endoscopic gastrostomy tube 33 days after the hemorrhage. At that time, GCS was 8 and the patient was bedridden, requiring constant nursing care and attention (modified Rankin score [mRS] 5). At the follow-up examination 6 months after hemorrhage, he showed a score of 2 on the extended Glasgow Outcome Scale (eGOS), and mRS was 5. Subsequently, the patient was readmitted to hospital for a generalized status epilepticus and treated with levetiracetam and lamotrigine.

Results

Neuromonitoring of SDs

ECOG monitoring started on day 1 after the initial hemorrhage, and lasted until day 12. Total recording time was 248.4 h. The predominant baseline activity was a burst-suppression pattern, possibly related to the continuous sedation with propofol. During the monitoring, 118 SDs were detected, resulting in a total depression time of 49.8 h. Fifty-four of the 118 SDs were isoelectric. In two cases, epileptic field potentials occurred on the final shoulder of the large slow potential change of SD, typical of spreading convolution (Dreier et al., 2012). In the near-DC recordings, the median amplitude of the slow potential change was 2.3 (1.7, 3.6) mV. Most SDs ran from electrode 6 to 5 to 3. Due to technical problems, electrode 4 was not recording. The median SD propagation velocity was 2.7 (2.0, 3.4) mm/min (median [first, third quartile]) assuming an ideal linear spread along the electrode strip. Levels of cerebral perfusion pressure (CPP), MAP, ICP, and $p_{ti}O_2$ at SD onset are given in Table 1.

$p_{ti}O_2$ was recorded in 79 SDs. Seventeen (21.5%) SDs displayed a hyperoxic response from 21.3 (16.8, 29.1) to 26.6 (20.2, 30.8) mm Hg, 23 (29.1%) SDs a hypoxic response from 24.0 (17.7, 30.0) to 22.5 (16.3, 28.8) mm Hg, followed by hyperoxia to 27.9 (20.3, 30.9) mm Hg, and 39 (49.4%) were not associated with any significant change in $p_{ti}O_2$.

rCBF was recorded with at least one of the optodes 3–6 in 76 SDs. At optode 3, we recorded 27 hyperemic rCBF responses (rCBF increase by 40.0% [22.3, 54.8]). At optode 4, 10 hyperemic (rCBF increase by 43.5% [38.0, 51.0]) and 5 hypoemic responses (rCBF decrease by 15.0% [24.3, 8.5]) were recorded. At optode 5, 13 hyperemic (increase by 33% [25.8, 40.3]) and 41 hypoemic responses (decrease by 12.0% [16.0, 8.8]) were recorded. Optode 6 showed 13 hyperemic responses with a median increase by 31.0% (28.8, 39.5).

Figure 1 displays the four initial SDs of a cluster. The first SD induced a persistent depression of spontaneous activity (i.e., spontaneous activity did not recover between the subsequent SDs). These subsequent SDs are therefore called isoelectric SDs. Although the first two SDs essentially showed hyperoxic responses, the third one demonstrated a hypoxic response. In a similar fashion, optode 5 first displayed two shallow hyperemic responses but the third response was hypoemic. No significant change of CPP was observed during this recording period (data not shown). Electrode 3 displayed only one SD. At optode 3, this SD was associated with a hyperemic response.

Neuromonitoring of ictal epileptic activity

In addition, we detected 31 events of isolated ictal epileptic activity resulting in a total duration of 7.0 h with ictal epileptic activity. In 16 of these events, the onsets of ictal epileptic activity occurred between different electrodes with such a delay that it remained somewhat unclear whether they represented only one or two separate ictal epileptic events. The median amplitude of the slow potential change containing ictal epileptic field potentials was 845 (720, 983) μ V. In contrast to the SDs that ran from electrode 6 toward 3, the ictal epileptic events ran from electrode 3 toward 6. The latter had a propagation velocity of 4.0

(2.2, 4.9) mm/min, assuming an ideal linear spread along the recording strip. Levels of CPP, MAP, ICP, and $p_{ti}O_2$ at the onset of ictal epileptic activity are given in Table 1.

$p_{ti}O_2$ recordings were available during the first 27 ictal epileptic events. A hyperoxic $p_{ti}O_2$ response from 18.0 (16.2, 19.1) to 27.7 (24.5, 29.4) mm Hg was detected in 25 (92.6%) events, whereas $p_{ti}O_2$ was “uncoupled” in two events (7.4%). No hypoxic responses were coupled to any of the ictal epileptic events. rCBF responses were recorded at optodes 3, 5, or both, in 22 ictal epileptic events. At optode 3, all of the 18 responses were hyperemic (rCBF increase by 57.0% [30.0, 82.0]). Of interest, at optode 5, all 10 rCBF responses were hypoemic (rCBF decrease by 12.0% [13.0, 9.0]).

Figure 2 displays an ictal epileptic event that propagated from electrodes 3–6. At optode 3, rCBF and $p_{ti}O_2$ show a hyperemic and hyperoxic response, respectively, whereas optode 5 displays a shallow rCBF decrease in a similar fashion to the previous rCBF response to SD at this optode (compare Fig. 1). Of note, the low-frequency vascular fluctuations (LF-VF) display a spreading suppression in a similar fashion to that of SDs.

Of interest, the quantitative analysis of the Gd-DTPA enhanced MRI on day 15 displayed a relatively selective BBB dysfunction in the vicinity of optoelectrodes 4 and 5 (Fig. 3A, B). Figure 3C gives the number of SDs and ictal epileptic events per day recording time after the initial hemorrhage. Of interest, the incidence of SDs showed an early peak on day 2, whereas ictal epileptic activity peaked on day 8.

Discussion

In acute brain injuries, the co-occurrence of SDs and ictal epileptic events can be differentiated into at least four patterns of interaction, as described previously (Fabricius et al., 2008). Herein we described a patient with aSAH in whom clusters of SDs preceded a status epilepticus during the course of the monitoring. The status epilepticus in this case thus seemed to “replace” the SDs. This is closely related to pattern II of the aforementioned study. The gap in time between the appearance of SDs and the appearance of ictal epileptic activity is interesting because previous findings suggested that SDs may cause BBB dysfunction (Gursoy-Ozdemir et al., 2004), BBB dysfunction may cause epilepsy (Friedman et al., 2009; Shlosberg et al., 2010; Stanićirović & Friedman, 2012), and a high frequency of SDs early in the course after aSAH was associated with a higher risk for the development of late epileptic seizures (Dreier et al., 2012). In the present case, BBB dysfunction has been documented for the first time in association with the transition from SDs to late epilepsy after brain injury. Whether this pathophysiologic cascade may play a significant role in postinjury epileptogenesis deserves further study.

Moreover, rCBF was recorded here for the first time in such a patient. The rCBF responses were in fact informative, since optodes 4 and 5 displayed hypoemic responses during SD unlike the normal hyperemic rCBF responses. Notably, at optode 5, rCBF was also recorded during the status epilepticus and showed remarkably similar hypoemic responses. In the spectrum from normal to inverse rCBF responses to SD (Dreier et al., 1998; Offenhauser et al., 2011), the hypoemic pattern at optodes 4 and 5 described herein was clearly abnormal in contrast to the normal patterns observed at optodes 3 and 6. Nevertheless, the hypoemic pattern did not fulfill the criteria for spreading ischemia because the blood flow reductions were only mild and shallow. Furthermore, they did not lead to any significant prolongation of the SD-identifying negative DC shifts at the corresponding electrode (Dreier et al., 2009; Dreier, 2011). The similarities between the hypoemic responses to SDs and the hypoemic responses to ictal epileptic events in this patient let us speculate that the underlying mechanisms were possibly related in this case. By contrast, there is good experimental

evidence that at least some of the mechanisms underlying full-blown spreading ischemia are SD specific. This applies in particular to the vasoconstrictive role of potassium that remains in the vasodilative concentration range during ictal epileptic activity, while it reaches the vasoconstrictive concentration range during SD (Windmuller et al., 2005).

Of note, the hypoemic responses were locally restricted to optodes 4 and 5, where the MRI detected a BBB dysfunction on day 15. This lets us speculate that the hypoemic responses could have some relation with the observed BBB dysfunction. Unfortunately, the temporal relationship between BBB dysfunction and the hypoemic responses remained unclear because the MRI scan was performed only after the rCBF recordings, on days 11 and 15 after the initial hemorrhage. Therefore, we do not know whether the BBB dysfunction preceded or followed the recorded SDs and ictal epileptic events. There was, however, consistency in the findings of the two MRI scans.

Another interesting aspect of this case was that ictal epileptic events were associated with spreading suppressions of LF-VFs. LF-VFs can be detected noninvasively with methods that record surrogate measures for rCBF such as near-infrared spectroscopy (NIRS) or functional MRI (fMRI). It is assumed that LF-VFs arise from the resting neuronal activity (Fox & Raichle, 2007). Consistently, it was found that the SD-induced spreading depression of spontaneous activity was associated with spreading suppression of LF-VFs in aSAH patients. Based on this observation, it was proposed that spreading suppression of LF-VFs may provide the option for noninvasive recordings of SDs using NIRS or fMRI (Dreier et al., 2009). But, if the present results can be reproduced and similar spreading suppressions of LF-VFs also accompany ictal epileptic events, it may be difficult to distinguish between SDs and ictal epileptic events with NIRS or fMRI. To overcome this problem, these noninvasive technologies could be combined with scalp electroencephalographic (EEG) recordings. Scalp EEG recordings are noninvasive in a similar fashion to NIRS and fMRI, and they were recently found to display correlates of SDs, which are clearly different from those of ictal epileptic events (Drenckhahn et al., 2012).

Acknowledgments

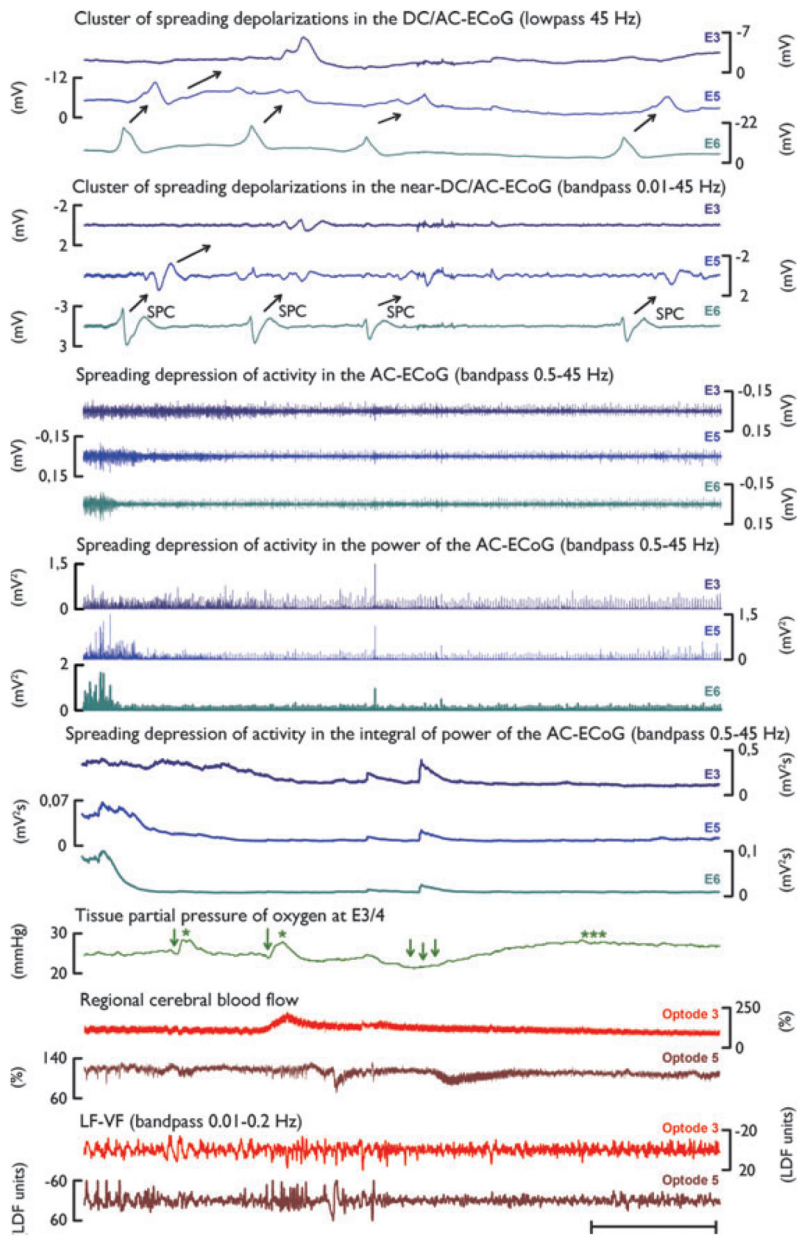
Supported by grants of the Deutsche Forschungsgemeinschaft (DFG Tr3 D10, DFG DR 323/5-1), the Bundesministerium für Bildung und Forschung (Center for Stroke Research Berlin 01 EO 0801 and Bernstein Center for Computational Neuroscience Berlin 01GQ1001C B2) and German Israeli Foundation (GIF) No. 124/2008. M. Scheel was supported by the “Friedrich C. Luft” Clinical Scientist Pilot Program funded by Volkswagen Foundation and Charité Foundation.

References

- Abbott NJ, Ronnback L, Hansson E. Astrocyte-endothelial interactions at the blood-brain barrier. *Nat Rev Neurosci.* 2006; 7:41–53. [PubMed: 16371949]
- Attwell D, Iadecola C. The neural basis of functional brain imaging signals. *Trends Neurosci.* 2002; 25:621–625. [PubMed: 12446129]
- Bosche B, Graf R, Ernestus RI, Dohmen C, Reithmeier T, Brinker G, Strong AJ, Dreier JP, Woitzik J. Recurrent spreading depolarizations after SAH decrease oxygen availability in human cerebral cortex. *Ann Neurol.* 2010; 67:607–617. [PubMed: 20437558]
- Buczacki SJ, Kirkpatrick PJ, Seeley HM, Hutchinson PJ. Late epilepsy following open surgery for aneurysmal subarachnoid haemorrhage. *J Neurol Neurosurg Psychiatry.* 2004; 75:1620–1622. [PubMed: 15489400]
- Butzkueven H, Evans AH, Pitman A, Leopold C, Jolley DJ, Kaye AH, Kilpatrick CJ, Davis SM. Onset seizures independently predict poor outcome after subarachnoid hemorrhage. *Neurology.* 2000; 55:1315–1320. [PubMed: 11087774]

- Claassen J, Peery S, Kreiter KT, Hirsch LJ, Du EY, Connolly ES, Mayer SA. Predictors and clinical impact of epilepsy after subarachnoid hemorrhage. *Neurology*. 2003; 60:208–214. [PubMed: 12552032]
- Dreier JP. The role of spreading depression, spreading depolarization and spreading ischemia in neurological disease. *Nat Med*. 2011; 17:439–447. [PubMed: 21475241]
- Dreier JP, Korner K, Ebert N, Gorner A, Rubin I, Back T, Lindauer U, Wolf T, Villringer A, Einhaupl KM, Lauritzen M, Dirnagl U. Nitric oxide scavenging by hemoglobin or nitric oxide synthase inhibition by N-nitro-L-arginine induces cortical spreading ischemia when K⁺ is increased in the subarachnoid space. *J Cereb Blood Flow Metab*. 1998; 18:978–990. [PubMed: 9740101]
- Dreier JP, Woitzik J, Fabricius M, Bhatia R, Major S, Drenckhahn C, Lehmann TN, Sarrafzadeh A, Willumsen L, Hartings JA, Sakowitz OW, Seemann JH, Thieme A, Lauritzen M, Strong AJ. Delayed ischaemic neurological deficits after subarachnoid haemorrhage are associated with clusters of spreading depolarizations. *Brain*. 2006; 129:3224–3237. [PubMed: 17067993]
- Dreier JP, Major S, Manning A, Woitzik J, Drenckhahn C, Steinbrink J, Tolias C, Oliveira-Ferreira AI, Fabricius M, Hartings JA, Vajkoczy P, Lauritzen M, Dirnagl U, Bohner G, Strong AJ. Cortical spreading ischaemia is a novel process involved in ischaemic damage in patients with aneurysmal subarachnoid haemorrhage. *Brain*. 2009; 132:1866–1881. [PubMed: 19420089]
- Dreier JP, Major S, Pannek HW, Woitzik J, Scheel M, Wiesenthal D, Martus P, Winkler MK, Hartings JA, Fabricius M, Speckmann EJ, Gorji A. Spreading convulsions, spreading depolarization and epileptogenesis in human cerebral cortex. *Brain*. 2012; 135:259–275. [PubMed: 22120143]
- Drenckhahn C, Winkler MKL, Major S, Scheel M, Kang EJ, Pinczolits A, Grozea C, Hartings JA, Woitzik J, Dreier JP. Correlates of spreading depolarizations in human scalp electroencephalography. *Brain*. 2012; 135:853–868. [PubMed: 22366798]
- Fabricius M, Fuhr S, Bhatia R, Boutelle M, Hashemi P, Strong AJ, Lauritzen M. Cortical spreading depression and peri-infarct depolarization in acutely injured human cerebral cortex. *Brain*. 2006; 129:778–790. [PubMed: 16364954]
- Fabricius M, Fuhr S, Willumsen L, Dreier JP, Bhatia R, Boutelle MG, Hartings JA, Bullock R, Strong AJ, Lauritzen M. Association of seizures with cortical spreading depression and peri-infarct depolarisations in the acutely injured human brain. *Clin Neurophysiol*. 2008; 119:1973–1984. [PubMed: 18621582]
- Fox MD, Raichle ME. Spontaneous fluctuations in brain activity observed with functional magnetic resonance imaging. *Nat Rev Neurosci*. 2007; 8:700–711. [PubMed: 17704812]
- Friedman A, Kaufer D, Heinemann U. Blood–brain barrier breakdown- inducing astrocytic transformation: novel targets for the prevention of epilepsy. *Epilepsy Res*. 2009; 85:142–149. [PubMed: 19362806]
- Gursoy-Ozdemir Y, Qiu J, Matsuoka N, Bolay H, Bermpohl D, Jin H, Wang X, Rosenberg GA, Lo EH, Moskowitz MA. Cortical spreading depression activates and upregulates MMP-9. *J Clin Invest*. 2004; 113:1447–1455. [PubMed: 15146242]
- Hartings JA, Bullock MR, Okonkwo DO, Murray LS, Murray GD, Fabricius M, Maas AI, Woitzik J, Sakowitz O, Mathern B, Roozenbeek B, Lingsma H, Dreier JP, Puccio AM, Shutter LA, Pahl C, Strong AJ. Spreading depolarisations and outcome after traumatic brain injury: a prospective observational study. *Lancet Neurol*. 2011a; 10:1058–1064. [PubMed: 22056157]
- Hartings JA, Watanabe T, Bullock MR, Okonkwo DO, Fabricius M, Woitzik J, Dreier JP, Puccio A, Shutter LA, Pahl C, Strong AJ. Spreading depolarizations have prolonged direct current shifts and are associated with poor outcome in brain trauma. *Brain*. 2011b; 134:1529–1540. [PubMed: 21478187]
- Heinemann U, Lux HD. Ceiling of stimulus induced rises in extracellular potassium concentration in the cerebral cortex of cat. *Brain Res*. 1977; 120:231–249. [PubMed: 832122]
- Kager H, Wadman WJ, Somjen GG. Conditions for the triggering of spreading depression studied with computer simulations. *J Neurophysiol*. 2002; 88:2700–2712. [PubMed: 12424305]
- Koehler RC, Roman RJ, Harder DR. Astrocytes and the regulation of cerebral blood flow. *Trends Neurosci*. 2009; 32:160–169. [PubMed: 19162338]
- Neuwelt EA, Bauer B, Fahlke C, Fricker G, Iadecola C, Janigro D, Leybaert L, Molnar Z, O'Donnell ME, Povlishock JT, Saunders NR, Sharp F, Stanimirovic D, Watts RJ, Drewes LR. Engaging

- neuroscience to advance translational research in brain barrier biology. *Nat Rev Neurosci.* 2011; 12:169–182. [PubMed: 21331083]
- Nortje J, Gupta AK. The role of tissue oxygen monitoring in patients with acute brain injury. *Br J Anaesth.* 2006; 97:95–106. [PubMed: 16751641]
- Offenbacher N, Windmuller O, Strong AJ, Fuhr S, Dreier JP. The gamut of blood flow responses coupled to spreading depolarization in rat and human brain: from hyperemia to prolonged ischemia. *Acta Neurochir Suppl.* 2011; 110:119–124. [PubMed: 21116926]
- Piilgaard H, Lauritzen M. Persistent increase in oxygen consumption and impaired neurovascular coupling after spreading depression in rat neocortex. *J Cereb Blood Flow Metab.* 2009; 29:1517–1527. [PubMed: 19513087]
- Shlosberg D, Benifla M, Kaufer D, Friedman A. Blood–brain barrier breakdown as a therapeutic target in traumatic brain injury. *Nat Rev Neurol.* 2010; 6:393–403. [PubMed: 20551947]
- Stanimirovic DB, Friedman A. Pathophysiology of the neurovascular unit: disease cause or consequence? *J Cereb Blood Flow Metab.* 2012; 32:1207–1221. [PubMed: 22395208]
- Sukhotinsky I, Yaseen MA, Sakadzic S, Ruvinskaya S, Sims JR, Boas DA, Moskowitz MA, Ayata C. Perfusion pressure-dependent recovery of cortical spreading depression is independent of tissue oxygenation over a wide physiologic range. *J Cereb Blood Flow Metab.* 2010; 30:1168–1177. [PubMed: 20087371]
- Tomkins O, Kaufer D, Korn A, Shelef I, Golan H, Reichenthal E, Soreq H, Friedman A. Frequent blood–brain barrier disruption in the human cerebral cortex. *Cell Mol Neurobiol.* 2001; 21:675–691. [PubMed: 12043841]
- Vespa PM, Nuwer MR, Nenov V, Ronne-Engstrom E, Hovda DA, Bergsneider M, Kelly DF, Martin NA, Becker DP. Increased incidence and impact of nonconvulsive and convulsive seizures after traumatic brain injury as detected by continuous electroencephalographic monitoring. *J Neurosurg.* 1999; 91:750–760. [PubMed: 10541231]
- Windmuller O, Lindauer U, Foddis M, Einhaupl KM, Dirnagl U, Heinemann U, Dreier JP. Ion changes in spreading ischaemia induce rat middle cerebral artery constriction in the absence of NO. *Brain.* 2005; 128:2042–2051. [PubMed: 15901647]
- Zhao M, Suh M, Ma H, Perry C, Geneslaw A, Schwartz TH. Focal increases in perfusion and decreases in hemoglobin oxygenation precede seizure onset in spontaneous human epilepsy. *Epilepsia.* 2007; 48:2059–2067. [PubMed: 17666071]

**Figure 1.**

Cluster of SDs over a period of 1 h on day 4 after aSAH. Traces 1–3 show the monopolar recordings of the DC-ECoG at electrodes 3, 5, and 6 in the frequency range below 45 Hz. Four SDs, identified by large, negative slow potential changes (SPCs) propagate from electrode 6 (E6) to electrodes 5 and 3 (E5, E3) (direction of propagation indicated by black arrows). Traces 4–6 show the parallel monopolar recordings of the near DC/AC-ECoG at electrodes 3, 5, and 6 in the frequency range between 0.01 and 45 Hz. Here again, black arrows point into the direction of propagation of the SDs. In the high-frequency, alternating current range of the ECoG (bandwidth 0.5–45 Hz), SD causes silencing of spontaneous activity, that is, spreading depression. This is observed as a rapid reduction in ECoG power. Traces 7–9 display the bandpass filtered ECoG recorded at electrodes 3, 5, and 6. The integral of power of the high frequency signal (traces 13–15) is used for visual enhancement of the amplitude loss and helps to determine the duration of the depression period beginning

at the initial decrease and ending at the start of the recovery, as described previously (Dreier et al., 2006). Note that the spreading depression of spontaneous activity propagates in a similar fashion as the SPCs from E6 to E3. Trace 16 displays changes in $p_{ti}O_2$, measured with the intraparenchymal oxygen sensor (see Methods section). Note that the first two SDs have essentially hyperoxic responses (green single asterisks, mild hypoxia indicated by green single arrows). The third SD causes a profound hypoxic response (triple arrows) followed by hyperoxia (triple asterisks). Optode 3 (trace 17) shows a hyperemic response to the SD recorded at electrode 3, whereas optode 5 displays a clearly hypoemic response to the third SD. This is coincident with the $p_{ti}O_2$ response described above. Note, however, that there is a delay in rCBF decrease after $p_{ti}O_2$ decrease. This is likely due to the spatial distance between the Licox probe (located between electrodes 3 and 4) and optode 5 (located near electrode 5).

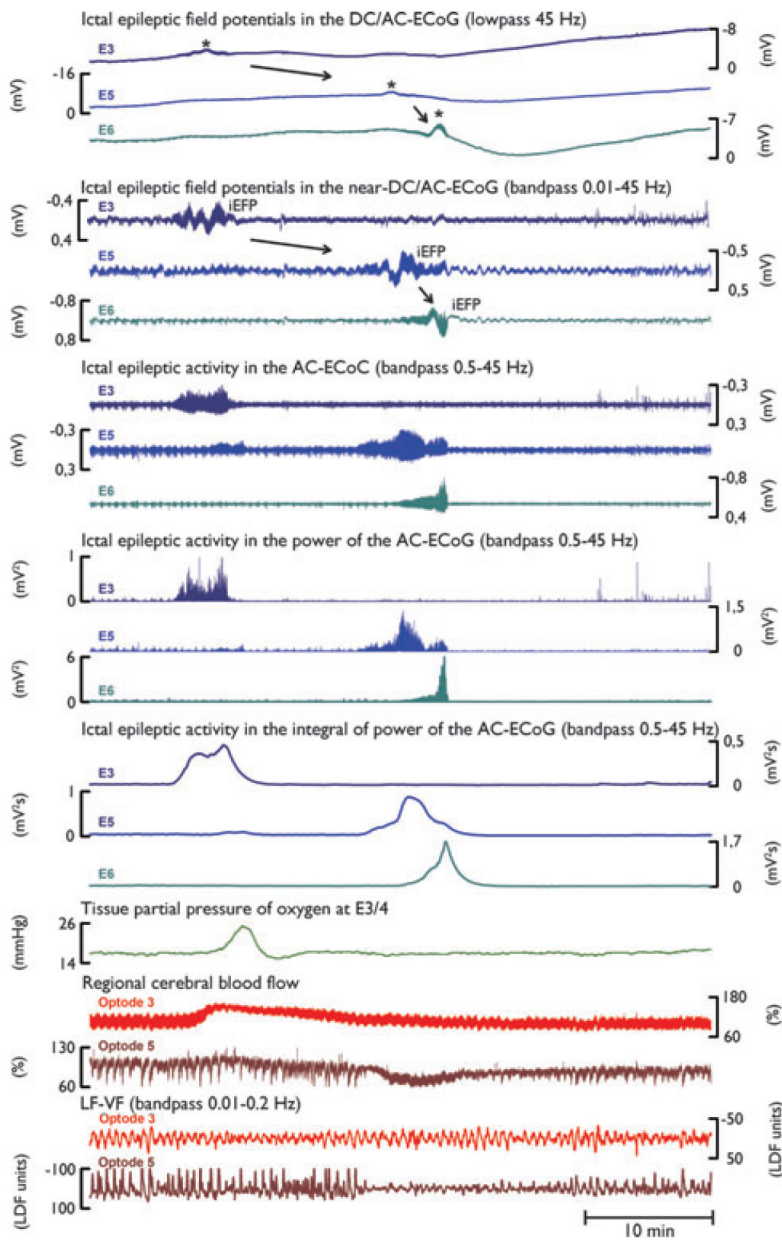
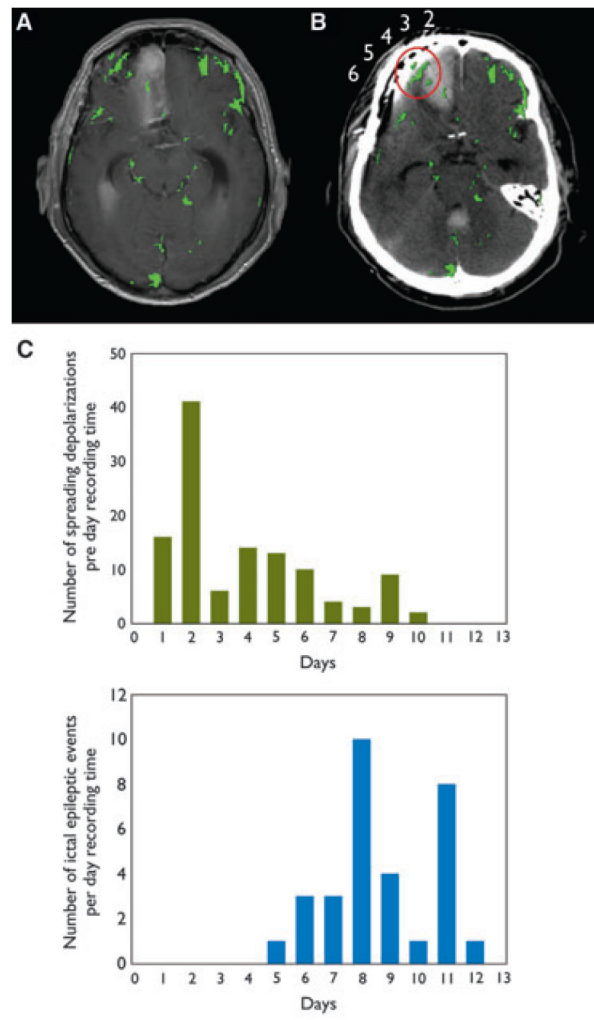


Figure 2.

Propagation of ictal epileptic activity during a recording period of 1 h on day 11 after aSAH. Here, ictal epileptic field potentials (iEFPs) (indicated by black asterisks in traces 1–6) coincide with sizable changes in the high-frequency AC-ECoG (bandwidth 0.5–45 Hz, displayed in traces 7–15). Similar to SD, ictal epileptic activity is associated with negative peaks in the DC/AC-ECoG but note that their amplitudes are much smaller than those of SDs. The amplitude of the spontaneous bandpass filtered high frequency ECoG activity (0.05–45 Hz) as well as the amplitudes of the power and the integral of the power show a sharp increase during ictal epileptic activity (traces 7–15) in contrast to SD where they show a decrease (depression) (compare Fig. 1). Also note that compared to SDs, ictal epileptic activity propagates in the opposite direction, from E3 to E5 to E6 (black arrows). P_{ti}O₂ (trace 16) shows a steep increase in tissue oxygenation in response to ictal epileptic activity. Traces 17–18 show changes in rCBF measured with optodes neighboring electrodes 3 and 5.

Although the rCBF response at optode 3 is hyperemic, optode 5 shows a shallow rCBF decrease in response to the ictal epileptic activity similar to the rCBF response to SD at optode 5 (compare Fig. 1). The two bottom traces demonstrate the parallel suppression of LF-VF (bandpass 0.01–0.2 Hz). Note that this suppression is similar to suppression of LF-VF during SD.

**Figure 3.**

Evaluation of BBB permeability. (A) Cerebral MRI scan on day 15 after aSAH shows BBB dysfunctional regions marked in green. (B) CT image showing the optoelectrode strip overlaid with the BBB findings of A. The tissue surrounding electrode 4 and 5 (circled in red) shows higher BBB permeability. To achieve registration between scans, MRI scan with highest correlation to the CT was rotated according to the skull orientation for maximum fit. Electrodes are positioned close to the skull, resulting in minor distortions between the models and allowing accurate overlay of findings. (C) Frequency distribution of SD and ictal epileptic events over 12 days of ECoG recording after aSAH. Two spreading convulsions that occurred on days 7 and 9 were counted as SDs. The incidence of SD has a peak on day 2 (41 SDs), whereas ictal epileptic events peak on day 8 (10 events). Highest co-occurrence of SD and ictal epileptic events is on days 5 (13 SDs, 1 ictal epileptic event), and 6 (10 SDs, three ictal epileptic events).

Table 1

Systemic parameters and tissue oxygen at the onset of SD and ictal epileptic activity

	CPP (mm Hg)	MAP (mm Hg)	ICP (mm Hg)	ptiO ₂ (mm Hg)
Values at SD onset	80.0 (75.7, 85.7)	97.0 (91.2, 99.8)	15.2 (11.5, 18.6)	22.4 (17.7, 29.2)
Values at onset of ictal epileptic activity	85.0 (75.8, 89.1)	99.0 (93.1, 102.7)	15.1 (11.2, 18.1)	18.7 (17.0, 20.5) ^a

^aOf interest, the ptiO₂ value at the onset of SDs was significantly higher than the ptiO₂ value at the onset of ictal epileptic events (n = 78 SDs, n = 28 ictal epileptic events, p-value = 0.003).